

$^{45}\text{Sc}(\alpha, d)^{47}\text{Ti}$ reaction*Gerald Hardie,[†] L. Meyer-Schützmeister, David Gloeckner,[‡] and T. H. Braid*Argonne National Laboratory, Argonne, Illinois 60439*

(Received 1 December 1975)

Using a split-pole magnetic spectrograph, the $^{45}\text{Sc}(\alpha, d)^{47}\text{Ti}$ reaction was studied at $E(\alpha) = 25$ MeV and with a range of angles from 7° to 50° . These measurements are compared with results we obtained using the $^{45}\text{Sc}(^3\text{He}, p)^{47}\text{Ti}$ reaction. One result of this comparison is the identification of candidates for states with high spin. The major emphasis of this paper is the study of such states. Two-particle spectroscopic amplitudes are calculated using an $(f_{7/2})^7$ model, assuming an inert ^{40}Ca core. Zero-range distorted-wave Born-approximation calculations are then performed with these amplitudes. A comparison between these shell-model calculations and the experimental results indicates that the states at 4.506 and 3.583 MeV have J^π 's of $19/2^-$ and $17/2^-$. A second result of the comparison between the (α, d) and $(^3\text{He}, p)$ reactions concerns the nature of the 3.22-MeV state in ^{47}Ti . It is strongly populated with an orbital angular momentum transfer of 0 by the $(^3\text{He}, p)$ reaction and only weakly populated by the (α, d) reaction, suggesting that it is formed by the transfer of a neutron-proton pair with $S = 0$, $T = 1$. This is similar to the transfer forming the state at 7.346 MeV, the analog of the ^{47}Sc ground state.

[NUCLEAR REACTIONS $^{45}\text{Sc}(\alpha, d)$, $E = 25$ MeV; measured $\sigma(\theta)$. ^{47}Ti deduced levels, J, π . Shell model and DWBA analyses.]

I. INTRODUCTION

Although the (α, d) and $(^3\text{He}, p)$ direct reactions both transfer an np pair, they have some differences which can be utilized in spectroscopic studies. In particular the (α, d) reaction, because of angular momentum mismatch between the entrance and exit channels, favors larger L transfers than the $(^3\text{He}, p)$ reaction (see Sec. II B). Consequently, the $^{45}\text{Sc}(\alpha, d)^{47}\text{Ti}$ reaction is expected to populate strongly states of high spin which are at most weakly populated by the $(^3\text{He}, p)$ reaction. Indeed, analysis of the measurements suggests several candidates for such states.

Another important difference between the (α, d) and $(^3\text{He}, p)$ reaction is the selection rules. In the (α, d) reaction, since the incident α particle has spin and isospin quantum numbers $S = 0$, $T = 0$ and the outgoing deuteron $S = 1$, $T = 0$, the np pair can only transfer $S = 1$, $T = 0$. However, both $S = 1$, $T = 0$ and $S = 0$, $T = 1$ transfers are possible with the $(^3\text{He}, p)$ reaction. In recent years it has been shown^{1,2} that, for the $(^3\text{He}, p)$ reaction with even-even targets, a $J^\pi = 1^+$ state is populated by an angular distribution with an orbital angular momentum transfer $L = 0 + 2$, except for a few cases³ of special nucleon configurations while, of course, a $J^\pi = 0^+$ state is excited by a pure $L = 0$ transfer. Hence an angular distribution characteristic of pure $L = 0$ signifies $S = 0$, $T = 1$ for the np pair and an angular distribution which contains a mixture of $L = 0$ and $L = 2$ indicates an $S = 1$, $T = 0$ np transfer. Similar $(^3\text{He}, p)$ results⁴ have

been observed for target nuclei with $J_i \neq 0$. Specifically, a pure $L = 0$ signifies an $S = 0$, $T = 1$ transfer with the population of $J_f^\pi = J_i^\pi$, $T = T_0$ or $T = T_0 + 1$ states, while $L = 0 + 2$ signifies an $S = 1$, $T = 0$ transfer with the population of $J_f^\pi = J_i^\pi$ or $J_f^\pi = J_i^\pi \pm 1$, $T = T_0$ states. The rules for the $(^3\text{He}, p)$ reaction and a comparison between the cross sections with which the (α, d) and $(^3\text{He}, p)$ reactions populate states in ^{47}Ti will be used to determine the properties of these states.

The results of the (α, d) study will be compared with shell-model calculations in which two-particle spectroscopic amplitudes are obtained using $f_{7/2}$ -model wave functions. These amplitudes are then used in a distorted-wave Born approximation (DWBA) calculation with the code TWOPAR.⁵ In particular, the relative cross sections with which high-spin states are populated will be compared with the shell-model predictions.

II. EXPERIMENTAL PROCEDURES AND RESULTS

A. Energy levels in ^{47}Ti

The $^{45}\text{Sc}(\alpha, d)^{47}\text{Ti}$ reaction was studied with a 25-MeV α -particle beam from the Argonne FN tandem Van de Graaff accelerator. The emergent deuterons were momentum analyzed by a split-pole magnetic spectrograph and then detected by Kodak NTB emulsions 50- μm thick, covered with acetate foils to stop some of the unwanted reaction products. These emulsions, after exposure and photographic development, were examined by an automatic nuclear-emulsion scanner.⁶ For deu-

teron groups the energy resolution was about 25 keV (FWHM), due mainly to energy losses in the target, a rolled ^{45}Sc foil of $140 \mu\text{g}/\text{cm}^2$ thickness. In Fig. 1 are shown spectra of deuterons emerging at angles of $\theta_{\text{lab}} = 22^\circ$ (upper spectrum) and $\theta_{\text{lab}} = 7^\circ$ (lower spectrum) with respect to the incident beam direction. In Table I are listed, for the level numbers in Fig. 1, the excitation energies and the cross sections at either 7° or 22° . Only levels which are well above the background at most angles are numbered. An exception is the one at $E_x = 3.23$ MeV (number 15). This level is not completely separated from the impurity *I*; consequently, the cross section can be measured only with a large uncertainty. The excitation energies given in column 2 of Table I are averages of those measured at the different angles. Levels 1 through 6 have an uncertainty of ± 0.010 MeV, while the others have an uncertainty of ± 0.015 MeV. These errors are sufficiently large to encompass a discrepancy we have noted (see p. 597 of Ref. 7) between energies measured with the spectrograph and with a Ge(Li) detector. More precise energies for some of the levels, obtained

from γ -ray work,⁷⁻⁹ are listed in column 7 of Table I. Also in Table I results obtained with the (α, d) reaction are compared with the excitation energies, cross sections and *L* values (columns 4-6) obtained with the $(^3\text{He}, p)$ reaction.⁷

To extend the above work to higher excitation energies in Ti, the (α, d) reaction on ^{45}Sc was studied at $\theta_{\text{lab}} = 20^\circ$ using a position-sensitive proportional counter in the focal plane of the split-pole magnetic spectrograph. Particle identification was used to obtain a spectrum containing only deuterons. This deuteron spectrum goes up to an excitation energy of 6.3 MeV. For energies below 4.8 MeV the results are the same as those obtained with emulsions. In the region from 4.8 to 6.3 MeV no deuteron groups were observed with intensities comparable to those populating states at 3.583 and 4.506 MeV (states numbered 18 and 24 in Table I).

B. Angular distributions

Deuterons from the $^{45}\text{Sc}(\alpha, d)$ reaction were detected with emulsions at 12 angles in the range

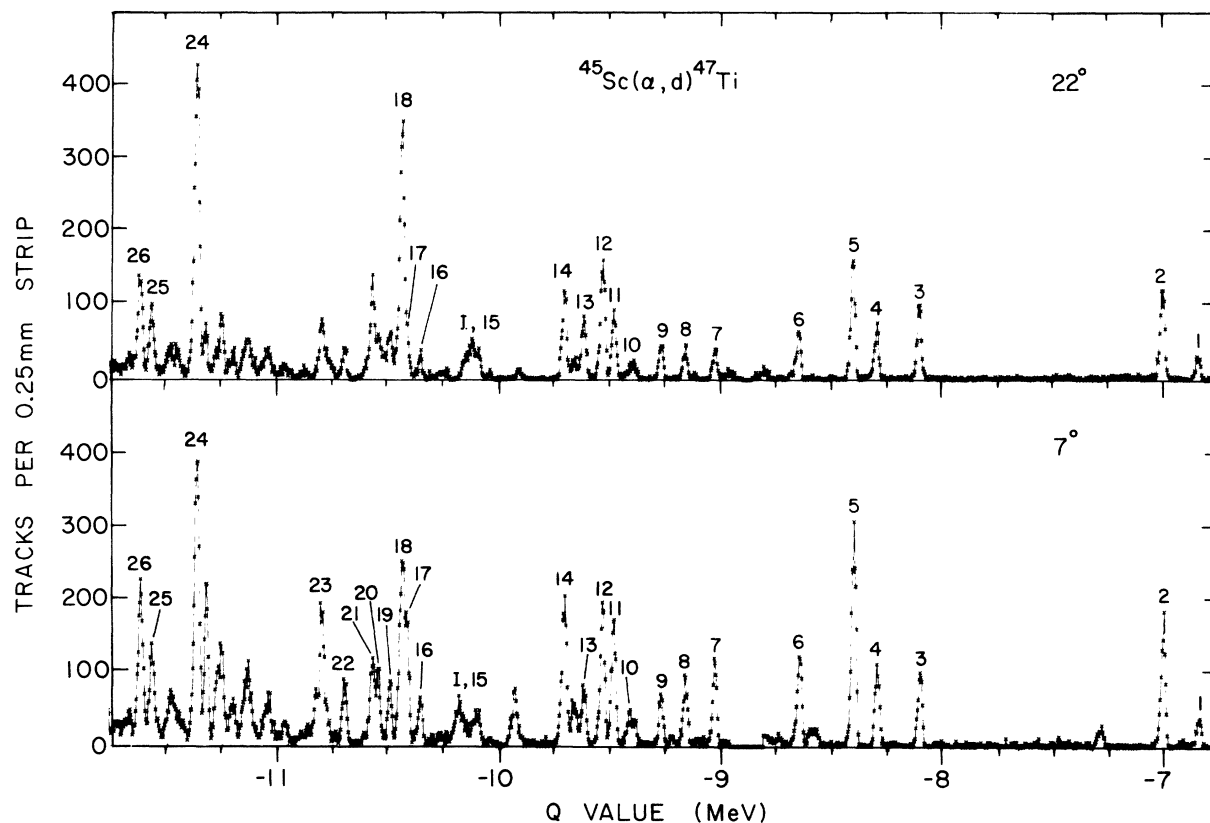


FIG. 1. Deuteron yield of the $^{45}\text{Sc}(\alpha, d)^{47}\text{Ti}$ reaction as a function of Q value. The spectra were obtained with the split-pole magnetic spectrograph at angles of 7° and 22° to the incident 25-MeV α -particle beam. The deuteron groups numbered correspond to states in ^{47}Ti and the excitation energies are listed in Table I.

TABLE I. Some experimental data on ^{47}Ti . The symbol $R = (d\sigma/d\omega)(\alpha, d)/(d\sigma/d\omega)(^3\text{He}, p)$. Level numbers refer to peaks in the spectrum shown in Fig. 1. All levels assigned spins have negative parities.

| Level No. | $^{45}\text{Sc}(\alpha, d)^a$ | | $^{45}\text{Sc}(^3\text{He}, p)^b$ | | L | γ ray studies ^c | | J^h | R |
|-----------|-------------------------------|---|------------------------------------|---|-----|-----------------------------------|--|------------------------------|---------------|
| | Ex. ^d (MeV) | $(d\sigma/d\omega)^e$ ($\mu\text{b}/\text{sr}$) ^{c.m.} | Ex. ^f (MeV) | $(d\sigma/d\omega)^e$ ($\mu\text{b}/\text{sr}$) ^{c.m.} | | Ex. ^g (MeV) | | | |
| 1 | 0.00 | 7 ± 1^i | 0.00 | 2.0 ± 0.5^i | (2) | | | $\frac{5}{2}$ | 3.5 ± 1.4 |
| 2 | 0.157 | 26 ± 2 | 0.150 | 6.4 ± 0.5 | 0+2 | 0.159 ± 0.001 | | $\frac{7}{2}$ | 4 ± 1 |
| 3 | 1.253 | 19 ± 2^i | 1.245 | $\leq 1^i$ | | 1.253 ± 0.001 | | $\frac{9}{2}$ | ≥ 19 |
| 4 | 1.446 | 18 ± 2 | 1.455 | 1.4 ± 0.5 | | 1.444 ± 0.002 | | $\frac{11}{2}$ | 13 ± 6 |
| 5 | 1.553 | 36 ± 3^i | 1.545 | 9 ± 1^i | 2 | 1.548 ± 0.002 | | $\frac{3}{2}$ | 4 ± 1 |
| 6 | 1.798 | 15 ± 2^i | 1.788 | 4.9 ± 0.6^i | 2 | 1.794 ± 0.002 | | $\frac{1}{2}$ | 3 ± 1 |
| 7 | 2.175 | 7 ± 1^i | 2.162 | 6.2 ± 0.5^i | 2 | 2.160 ± 0.002 | | $(\frac{1}{2}, \frac{3}{2})$ | 1.1 ± 0.2 |
| 8 | 2.31 | 15 ± 2 | | | | | | | |
| 9 | 2.42 | 11 ± 1 | | | | | | | |
| 10 | 2.54 | 6 ± 1 | 2.53 | 3.4 ± 0.5 | | | | $\frac{3}{2}$ | 1.8 ± 0.6 |
| 11 | 2.63 | 29 ± 2 | 2.61 | 14 ± 1 | 0+2 | 2.614 ± 0.004 | | $\frac{7}{2}$ | 2.1 ± 0.3 |
| 12 | 2.68 { | 33 ± 2 { | | ≤ 1 { | | 2.672 ± 0.001 | | $\frac{13}{2}$ | ≥ 33 { |
| | | | | | | 2.684 ± 0.002 | | $(\frac{11}{2})^j$ | |
| 13 | 2.77 | 16 ± 2^i | | $\leq 4^i$ | | 2.748 ± 0.002 | | $\frac{15}{2}$ | ≥ 4 |
| 14 | 2.85 | 39 ± 2 | 2.84 | 42 ± 4 | 0+2 | 2.835 ± 0.004 | | $(\frac{5}{2})$ | 0.9 ± 0.1 |
| 15 | 3.23 | < 4 | 3.22 | 20 ± 2 | 0 | 3.223 ± 0.004 | | $\frac{7}{2}$ | < 0.2 |
| | | | | | | 3.289 ± 0.001 | | $(\frac{13}{2})^j$ | |
| 16 | 3.50 | 10 ± 1 | | | | | | | |
| 17 | 3.56 | 30 ± 2 | | | | | | | |
| 18 | 3.58 | 68 ± 3^i | | $\leq 2^i$ | | 3.567 ± 0.005 | | $\frac{17}{2}$ | ≥ 34 |
| 19 | 3.64 | 13 ± 1 | | | | | | | |
| 20 | 3.69 | 17 ± 1 | | | | | | | |
| 21 | 3.72 | 20 ± 2^i | | | | | | | |
| 22 | 3.84 | 10 ± 1 | | | | | | | |
| | | | 3.92 | 6 ± 1^i | 2 | 3.913 ± 0.006 | | $\frac{3}{2}$ | |
| 23 | 3.95 | 31 ± 2 | | | | | | | |
| 24 | 4.51 | 92 ± 7^i | 4.50 | 6 ± 2^i | | 4.494 ± 0.005 | | $\frac{19}{2}$ | 15 ± 6 |
| 25 | 4.71 | 18 ± 2 | 4.71 | 27 ± 3 | 0+2 | | | | 0.7 ± 0.2 |
| 26 | 4.76 | 37 ± 2 | 4.76 | 26 ± 3 | | | | | 1.4 ± 0.3 |

^aThis work.

^bReference 7.

^cReferences 7, 8, and 9.

^dLevels 1 through 6 have an uncertainty of ± 0.010 MeV, the others an uncertainty of ± 0.015 MeV.

^eValue at 7° (lab) unless otherwise noted.

^fThe energies shown have an uncertainty of ± 0.010 MeV for levels 1 through 15 and ± 0.015 MeV for the others. Those energies not listed are very uncertain.

^gDetermined from measured γ ray energies.

^hSee references 7, 8, 9, and 12 and references contained therein, as well as present work.

ⁱValue at 22° (lab).

^jUncertain spins (see Refs. 9 and 8).

$\theta_{\text{lab}} = 7^\circ$ to 50° . The angular distributions are displayed in Figs. 2-5 for all the states listed in Table I. In contrast to the proton angular distributions from the $(^3\text{He}, p)$ reaction, these deuteron angular distributions have little structure, most of them decreasing smoothly with increasing angle. As examples, the proton and deuteron angular distributions for the 1.55- and 2.61-MeV states are given in Fig. 6. The two proton angular distributions differ greatly, one characteristic of $L = 2$ ($E_x = 1.55$ MeV) and the other of $L = 0 + 2$. On the other hand, the deuteron angular distributions differ only slightly. The difference between the shapes of the proton and deuteron angular distributions is due to the fact that the two reactions have quite different kinematics, thus favoring different L transfers. In particular, the (α, d) reaction is much more favorable for transfers with large L values than is the $(^3\text{He}, p)$ reaction. This fact is shown in Table II, which lists the relative

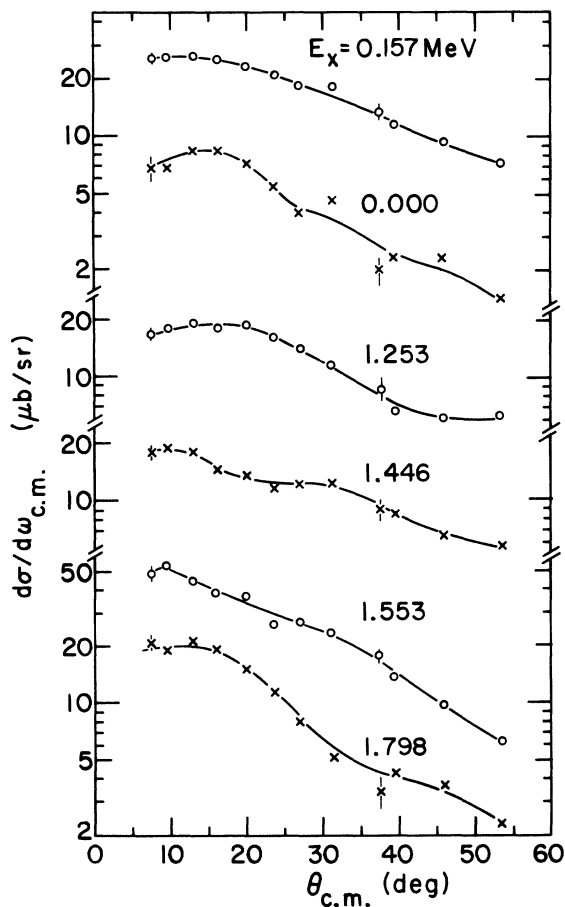


FIG. 2. Angular distributions of deuterons from the $^{45}\text{Sc}(\alpha, d)^{47}\text{Ti}$ reaction. The energy of the beam was 25 MeV. The solid lines are curves to aid the eye.

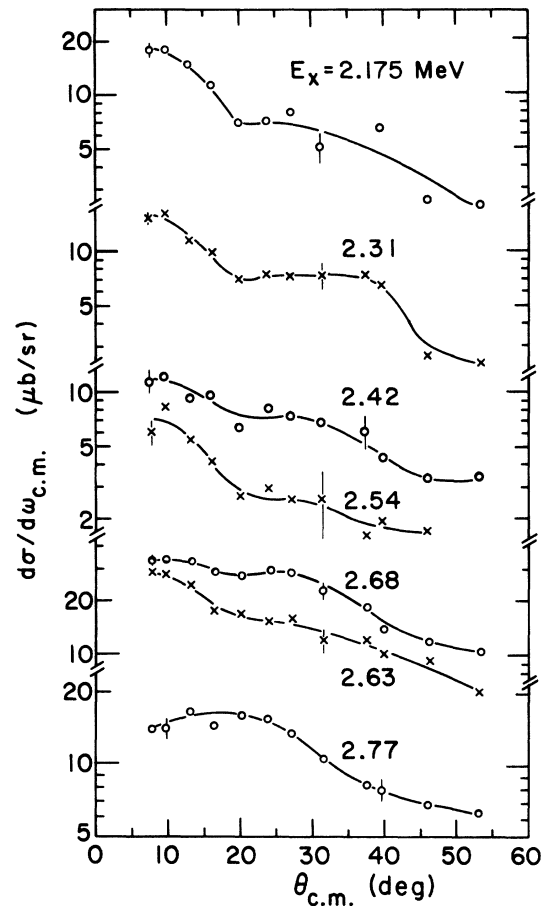


FIG. 3. Angular distributions of deuterons from the $^{45}\text{Sc}(\alpha, d)^{47}\text{Ti}$ reaction. The energy of the beam was 25 MeV. The solid lines are curves to aid the eye.

calculated cross sections for both reactions and their ratios $\sigma(\alpha, d)/\sigma(^3\text{He}, p)$. These calculations were made with the program TWOPAR using the potentials^{7,10,11} given in Table III and with both nucleons transferred to the $f_{7/2}$ shell. The values for σ are obtained by integrating the differential cross sections $[\int (d\sigma/d\omega) \sin\theta d\theta]$ over an angular range from 5° to 50° and normalizing to 1 for an $L = 0$ transfer. It is seen from Table II that states which are populated with $L = 4$ or 6 or both are 8 to 20 times more strongly excited relative to an $L = 0$ transfer by the (α, d) reaction than by the $(^3\text{He}, p)$ reaction. The ratios $R = \sigma(\alpha, d)/\sigma(^3\text{He}, p)$ are not very sensitive to the choice of potentials.

The angular distributions calculated for the deuterons leading to high-spin states with the (α, d) reaction show a broad maximum at about 20° , and are rather insensitive to small changes in the potentials given in Table III. Consequently, this characteristic shape for a deuteron angular

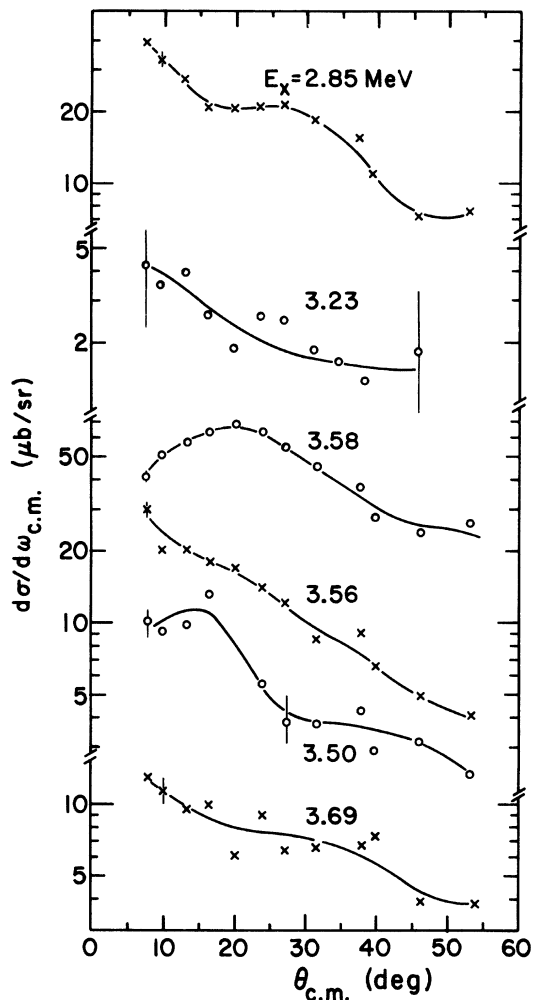


FIG. 4. Angular distributions of deuterons from the $^{45}\text{Sc}(\alpha, d)^{47}\text{Ti}$ reaction. The energy of the beam was 25 MeV. The solid lines are curves to aid the eye.

distribution (see Figs. 2 to 5) and a large value of R (see Table I) are criteria by which we select candidates for high-spin states. States with excitation energies of 1.253, 2.77, 3.58, and 4.51 MeV satisfy both criteria. The state at 1.253 MeV is known to be the $J^\pi = \frac{9}{2}^-$ yrast level (Table I). Two other states, at 1.446 and 2.68 MeV, have large values of R . The former is the $\frac{11}{2}^-$ yrast level (Table I). The latter will be considered a possible high-spin state. In addition, deuterons populating the state at 3.72 MeV have an angular distribution characteristic of a high-spin state, but we can provide no information about its spin and parity. Hence the states at 1.253, 1.446, 2.68, 2.77, 3.58, and 4.51 MeV seem to be populated by large L -value transfers, and indeed this work, combined with γ -ray investigations,^{7-9,12}

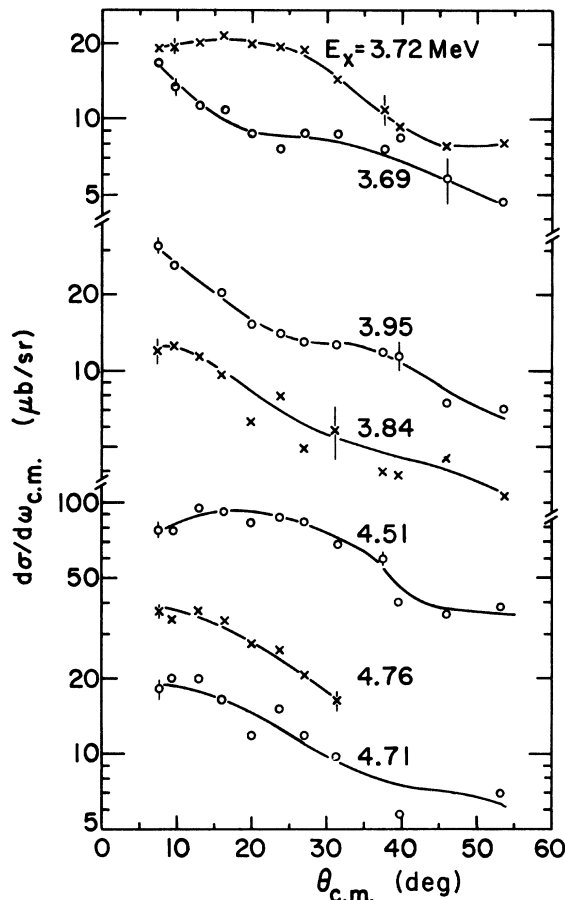


FIG. 5. Angular distributions of deuterons from the $^{45}\text{Sc}(\alpha, d)^{47}\text{Ti}$ reaction. The energy of the beam was 25 MeV. The solid lines are curves to aid the eye.

shows that they are yrast levels and have J^π 's of $\frac{9}{2}^-$, $\frac{11}{2}^-$, $\frac{13}{2}^-$, $\frac{15}{2}^-$, $\frac{17}{2}^-$, and $\frac{19}{2}^-$, respectively.

III. COMPARISON WITH THEORETICAL CALCULATIONS

A. $^{45}\text{Sc}(\alpha, d)^{47}\text{Ti}$ reaction

Several models^{7,13,14} have been used to describe ^{47}Ti . The Coriolis-coupling model of Malik and Scholz¹⁴ has been used to describe low-spin states. Dhar, Kulkarni, and Bhatt¹³ have performed truncated shell-model calculations with a basis generated from a deformed Hartree-Fock solution. We will compare the results of Dhar *et al.*¹³ with the experimental results and our $(f_{7/2})^7$ shell-model calculations. These shell-model calculations were performed assuming an inert ^{40}Ca core and two-body matrix elements (given in Ref. 15) obtained from the well-known spectrum of ^{42}Sc . They were used not only to calculate the level scheme of ^{47}Ti but, in addition, the spectroscopic

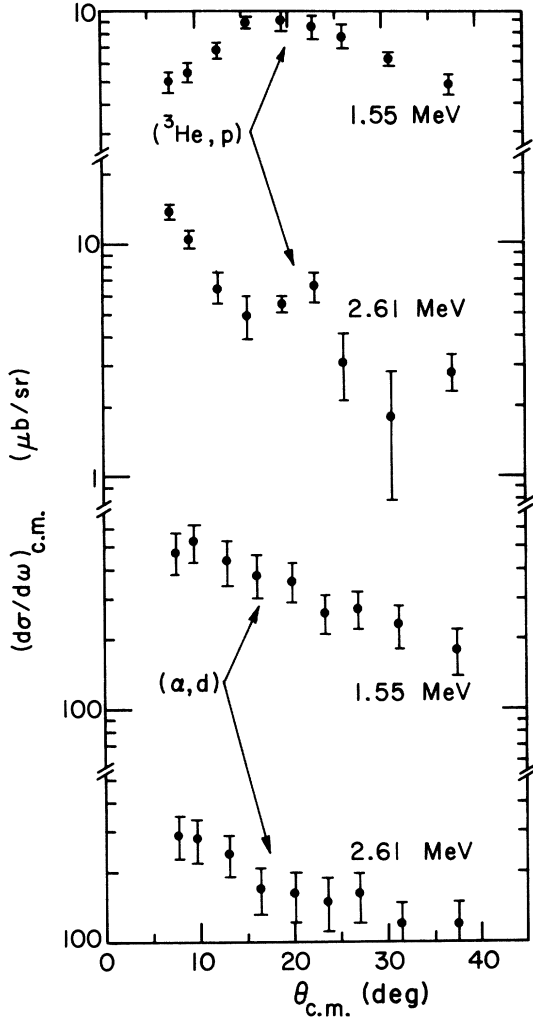


FIG. 6. Angular distributions of protons from the $^{45}\text{Sc}(^3\text{He}, p)^{47}\text{Ti}$ reaction and deuterons from the $^{45}\text{Sc}(\alpha, d)^{47}\text{Ti}$ reaction to states with excitation energies of 1.55 and 2.61 MeV. The upper and lower proton angular distributions are characteristic of $L=2$ and $L=0+2$ transfers, respectively.

amplitudes for populating the ^{47}Ti levels by the (α, d) reaction. Calculated angular distributions for the deuterons were then obtained by using these spectroscopic amplitudes in DWBA calculations performed with the zero-range code TWOPAR.⁵ The optical-model parameters chosen are given in Table III. Much more difficulty is encountered in fitting (α, d) than $(^3\text{He}, p)$ angular distributions, consequently results depending on the deuteron and α -particle optical-model parameters must be treated with caution. However, we have made calculations with four sets of potentials^{10, 11, 16-19} and found, for states with $J \geq \frac{9}{2}$, that $(d\sigma/d\omega)\sin\theta$ summed from 5° to 50° deviates from the average

TABLE II. The calculated relative cross sections and their ratios for the (α, d) and $(^3\text{He}, p)$ reactions on ^{45}Sc for different orbital angular momentum transfers (L). The potentials used in the DWBA calculations are given in Table III. The symbol σ represents the differential cross sections integrated over the angular range $5-50^\circ$ with respect to the beam direction. In the calculation for the $(^3\text{He}, p)$ reaction both spin singlet and triplet states were included, the singlet contribution being weighed by a factor of 3 (see Ref. 15).

| | $L=0$ | 2 | 4 | 6 |
|--|-------|------|------|-------|
| $\sigma(\alpha, d)$ | 1.0 | 0.63 | 0.93 | 1.78 |
| $\sigma(^3\text{He}, p)$ | 1.0 | 0.26 | 0.11 | 0.090 |
| $\sigma(\alpha, d)/\sigma(^3\text{He}, p)$ | 1.0 | 2.4 | 8.5 | 20 |

by less than 10%.

Comparison of experimental results with calculations has already been made^{7, 13, 20} for levels with low spins, $J \leq \frac{7}{2}$, using data from the $(^3\text{He}, p)$ reaction and one-nucleon transfer reactions. The present paper will emphasize the experimental and theoretical results for high-spin states. In Fig. 7 the results of our shell-model calculations and the calculations of Dhar *et al.*¹³ are compared with the observed locations of high-spin states. Both calculations predict such high-spin states at approximately the observed energies. The Hartree-Fock calculations give excitation energies in somewhat better agreement with the experimentally determined ones. However, the shell-model calculations can be considered quite satisfactory in view of the severe truncation. A more stringent test of these models will be the degree to which they can reproduce the observed electromagnetic decay of the high-spin states.

The deuteron angular distributions predicted by DWBA calculations are qualitatively different for states populated with large L transfers than for states reached by small L transfers. In Fig. 8 we have plotted the calculated angular distributions for the yrast levels with spins and parities of $\frac{9}{2}^-$, $\frac{11}{2}^-$, $\frac{13}{2}^-$, $\frac{15}{2}^-$, $\frac{17}{2}^-$, and $\frac{19}{2}^-$. Unlike the non-yrast levels, they are dominated by an $L=6$ transfer even though, with the exception of the $\frac{19}{2}^-$ state, conservation of angular momentum permits their population with a smaller L transfer. Shown for comparison are the experimentally observed angular distributions for states with excitation energies of 1.253, 1.446, 2.68, 2.77, 3.58, and 4.51 MeV which are assumed to be yrast levels. The agreement is satisfactory showing that these states are populated mainly by $L=6$ transfers even though, for $J \leq \frac{13}{2}$, $L=2$ is sufficient. That large L transfers are indeed favored for these

TABLE III. The optical potentials and parameters used in the DWBA calculations, in which the potential for the unbound particle is $V(r) = -Vf_v(r) - iWf_w(r) + 4ia_s W_s f'_s(r)$, where $f_x = \{1 + \exp[(r - r_x A^{1/3})/a_x]\}^{-1}$ and $f' = \partial f / \partial r$. The parameters of the potential in which the bound neutron and proton move are $a_v = 0.65$ fm and $r_v = 1.25$ fm. The program adjusts the real potential well until the binding energy is $E = \frac{1}{2}(|S_{np}| - E_x)$, where E_x is the excitation energy in the final nucleus and S_{np} is the separation energy of the n - p pair.

| Unbound particle | V (MeV) | a_v (fm) | r_v (fm) | W (MeV) | a_w (fm) | r_w (fm) | W_s (MeV) | a_s (fm) | r_s (fm) |
|-------------------|-----------|------------|------------|-----------|------------|------------|-------------|------------|------------|
| p^a | 53.6 | 0.61 | 1.217 | 0.0 | ... | ... | 17.1 | 0.31 | 1.26 |
| ${}^3\text{He}^a$ | 160 | 0.734 | 1.13 | 16.21 | 0.734 | 1.13 | 0.0 | ... | ... |
| d^b | 115.38 | 0.878 | 1.006 | 0.0 | ... | ... | 18.766 | 0.482 | 1.517 |
| α^c | 183.70 | 0.560 | 1.400 | 26.0 | 0.560 | 1.480 | 0.0 | ... | ... |

^a From Ref. 7.

^b From Ref. 10.

^c From Ref. 11.

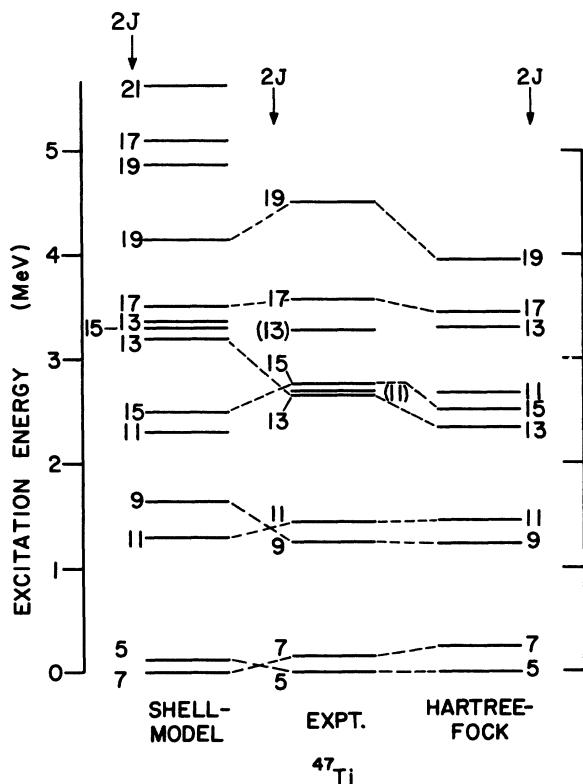


FIG. 7. Some negative-parity energy levels, mainly those having high-spin values, in ${}^{47}\text{Ti}$. The experimentally determined spectrum is from the present work and Refs. 8 and 9. Results from our $(f_{7/2})^7$ shell-model calculations are shown on the left. The Hartree-Fock calculations taken from Ref. 13 are shown on the right. The numbers at the level positions are $2J$ values. The spin assignments shown in brackets are in doubt (see Sec. IV).

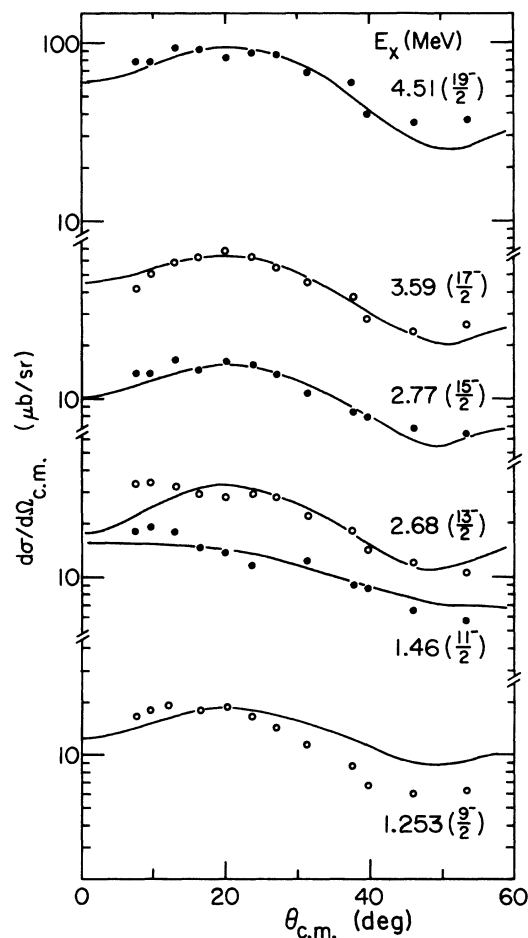


FIG. 8. A comparison of measured angular distributions of deuterons populating high spin states in ${}^{47}\text{Ti}$ with calculations using the $(f_{7/2})^7$ shell model. The curves are the result of DWBA calculations and have been normalized to the data.

states is indicated by their low production cross sections with the $(^3\text{He}, d)$ reaction, which favors small L transfers (see Table II). The angular distribution of the state at 2.68 MeV might contain some contribution from the 2.684-MeV state observed in γ -ray studies.^{8,9} Since the latter state is not a member of the yrast system of negative parity, its contribution compared to that of the $\frac{13}{2}^-$ state at 2.672 MeV is predicted to be small (see Fig. 9 and discussion below).

Additional evidence in support of the spin assignments is provided by a comparison of the calculated and the experimentally observed relative strengths for the population of the yrast levels by the (α, d) reaction. These relative strengths are obtained by integrating the differential cross sections in the range from 5° to 50° . The result is presented in Fig. 9, the first $\frac{19}{2}^-$ state being chosen for normalization. Also shown are the strengths to the first non-yrast high-spin states. For $J^\pi > \frac{9}{2}^-$ they are weaker than those to the yrast levels with the same J . In particular, the second $\frac{11}{2}^-$ state is predicted to be very weakly populated. Hence if the state at 2.684 MeV is the $\frac{11}{2}^-$ level,⁹ its contribution to the deuteron group at 2.68 MeV is probably small, and the dominant contribution results from the population of the $\frac{13}{2}^-$ state at 2.672 MeV. If the state at 2.684 MeV has positive parity,⁸ it presumably has a nucleon configuration with a large $d_{3/2}$ hole component. Since this com-

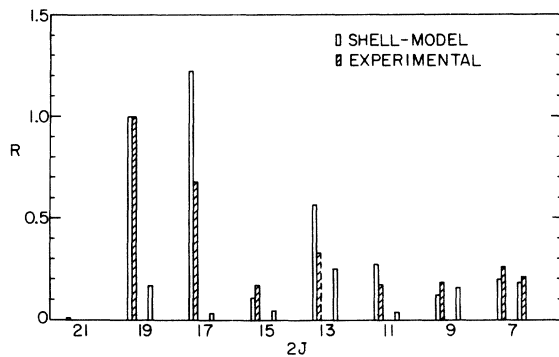


FIG. 9. A comparison between shell-model calculations and experimental results of the relative strengths for populating negative-parity states in ^{47}Ti by the (α, d) reaction. The open bars are the result of a calculation with an $(f_{7/2})^7$ shell model. The hatched bars are the experimental results. For each J value, the bars on the left are for the yrast levels and the ones on the right are for the first non-yrast levels. The symbol R is:

$$R = \left\{ \frac{\int_{5^\circ}^{50^\circ} \left(\frac{d\sigma}{d\omega} \sin\theta \right)^J d\theta}{\int_{5^\circ}^{50^\circ} \left(\frac{d\sigma}{d\omega} \sin\theta \right)^{19/2} d\theta} \right\}.$$

ponent is assumed to be small in the target nucleus the excitation of this state by the (α, d) reaction is expected to be small. Agreement of the strengths calculated using the shell model with those experimentally observed is good, as shown in Fig. 9. In particular it should be noted that, experimentally, the strength to the $\frac{15}{2}^-$ state is only 0.17 times that to the $\frac{19}{2}^-$ state, a fact accounted for in the calculations. In addition, the fact that no state above the $\frac{19}{2}^-$ yrast level is populated with a large cross section is also predicted by the calculations. In particular, the $\frac{21}{2}^-$ yrast state is expected to be populated only weakly (see Fig. 9). On the other hand, the theory predicts a rather large cross section for populating the first non-yrast $\frac{13}{2}^-$ state by the (α, d) reaction. This state is reported⁹ to be at 3.289 MeV, a state we do not populate, and hence we would conclude that either the $\frac{13}{2}^-$ assignment is incorrect,⁸ or that the $f_{7/2}$ shell model is not as successful for the non-yrast as for the negative-parity yrast states.

A discrepancy between the shell-model calculations and the experimental results is observed in the cross sections for populating the $\frac{17}{2}^-$ and $\frac{19}{2}^-$ yrast levels. As seen in Fig. 9, the $\frac{19}{2}^-$ state is observed to be more strongly populated than the $\frac{17}{2}^-$ state, while the theoretical prediction is just the opposite. An attempt was made to reduce this discrepancy by enlarging the shell-model space to permit one nucleon in either the $f_{5/2}$, $p_{3/2}$, or $p_{1/2}$ subshell. For this model we used modified Kuo-Brown matrix elements.²¹ In addition, a Coulomb interaction, calculated with harmonic oscillator wave functions and $\hbar\omega = (41/A^{1/3})$ MeV, was added to the proton-proton matrix elements. The single particle energies were taken from data in the $A = 40$ mass region.²² In this model there is coherent addition for a $J = 5$ transfer of the $f_{7/2}f_{7/2}$ and $f_{7/2}f_{5/2}$ amplitudes to the $\frac{17}{2}^-$ state. However, there is only the incoherent sum of the $f_{7/2}f_{7/2}J = 7$ and $f_{7/2}f_{5/2}J = 6$ amplitudes to the $\frac{19}{2}^-$ state. The result of the calculation is that there is destructive interference in the $J = 5$ transfer to the $\frac{17}{2}^-$ state, but the reaction is still dominated by the $J = 7$ transfer for which no interference is possible. Since the $J = 7$ transfer to the $\frac{17}{2}^-$ state is larger than to the $\frac{19}{2}^-$ state, this model does not remove the discrepancy.

Finally, it should be emphasized that our work using a position-sensitive proportional counter (see Sec. IIA) has shown that the deuteron groups populating the levels at 3.58 and 4.51 MeV have the largest cross sections for all excitation energies up to 6.3 MeV. This fact strongly suggests, independently of the γ -ray work, that these two levels are the yrast states with spins and parities of $\frac{17}{2}^-$ and $\frac{19}{2}^-$.

B. 3.223-MeV state

Only two states in ^{47}Ti are populated by the ($^3\text{He}, p$) reaction with a predominant $L = 0$ transfer.⁷ One state, the analog of the ground state of ^{47}Sc , is at 7.346 MeV and the other is at 3.223 MeV. The 3.223-MeV state is populated only weakly by the (α, d) reaction. Hence not only the analog state but also the 3.223-MeV state is dominated in a two-nucleon transfer reaction by the component

$$\{[(f_{7/2})^2_{J=0, T=1}] \times |^{45}\text{Sc}(\text{g.s.})\}_{T},$$

where $T = T_>$ for the analog and $T = T_<$ for the 3.223-MeV state.

The $f_{7/2}$ -shell model does not predict a state dominated by a $J = 0$ transfer in the ($^3\text{He}, p$) reaction. While the model contains sufficient strength for populating $\frac{7}{2}^-$ states with a $J = 0$ transfer, a significant fraction of the sum-rule strength goes with $J > 0$ regardless of which $\frac{7}{2}^-$ model state is considered as a candidate for the 3.223-MeV state. Hence there is no model state with $J^\pi = \frac{7}{2}^-, T = T_<$ populated by a predominant $J = 0$ transfer. There appears little likelihood that changes in the two-body matrix elements will result in the prediction of such a state. Unfortunately, for $J^\pi \neq 0$ targets, no other case of a $T_<$ state populated by a predominant $S = 0, T = 1$ transfer is known in which the transferred nucleons go into a partially occupied valence shell ($f_{7/2}$ in this case). For example, no such state is populated in ^{45}Sc by the ($^3\text{He}, p$) reaction on ^{43}Ca . One might be tempted to consider the 3.223-MeV state the "antianalog" corresponding to the 7.346-MeV analog state, since these are the only two states strongly populated by a $T = 1$ transfer. However, since no such state can be obtained theoretically, the nature of the 3.223-MeV state, and its relationship to the analog, is not clear.

IV. SUMMARY

A comparison of the results from the (α, d) and ($^3\text{He}, p$) reactions to the same final nucleus can

provide important spectroscopic information. For example, we have shown from such a comparison that the 3.223-MeV state in ^{47}Ti is reached by transferring a neutron-proton pair with $T = 1$. It is the only $T_<$ state populated in this manner. However, no such state is predicted by an ($f_{7/2}$)⁷ shell model.

We have compared results obtained from an $f_{7/2}$ -shell model with the properties of states in ^{47}Ti at excitation energies of 0.57, 1.253, 1.446, 2.68, 2.77, 3.58, and 4.51 MeV. This comparison confirms these states as members of the yrast system with J^π 's of $\frac{7}{2}^-, \frac{9}{2}^-, \frac{11}{2}^-, \frac{13}{2}^-, \frac{15}{2}^-, \frac{17}{2}^-,$ and $\frac{19}{2}^-$. As expected from the calculations the $\frac{21}{2}^-$ yrast level was not identified.

The states at 2.684 and 3.289 MeV are not members of the negative parity yrast system and have been assigned⁹ spins and parities of $\frac{11}{2}^-$ and $\frac{13}{2}^-$, respectively. In contrast to levels of the negative parity yrast system, the γ decay of these two states^{8,9} is not correctly predicted by the $f_{7/2}$ -shell model. This means that either the $f_{7/2}$ -shell model is reliable only for the high-spin yrast system (negative parity), or that the spin and parity assignments of the two levels are incorrect. There is indeed strong evidence⁸ that the 2.684-MeV state has $J^\pi = \frac{7}{2}^+$ or $\frac{11}{2}^+$. Since the spin assignment of the 3.289-MeV state is based on the one of the 2.684-MeV state it is presumably also incorrect. Hence it is possible that the $f_{7/2}$ shell-model calculations are not only able to predict the yrast levels of high negative spin but also high-spin states of negative parity which do not belong to the yrast system.

ACKNOWLEDGMENTS

We would like to acknowledge many helpful discussions with D. Kurath and J. Schiffer. We are also grateful to F. G. Karasek of the Materials Science Division of the Argonne National Laboratory for preparing the rolled target.

*Work performed under the auspices of the U. S. Energy Research and Development Administration.

†Also at Physics Department, Western Michigan University, Kalamazoo, Michigan 49001.

‡Also at Physics Department, Rutgers University, New Brunswick, New Jersey, 08903.

¹R. R. Betts, H. T. Fortune, J. D. Garrett, R. Middleton, and D. J. Pullen, Phys. Rev. Lett. **26**, 1121 (1971).

²J. W. Smith, L. Meyer-Schützmeister, and Gerald Hardie, Phys. Rev. C **8**, 2232 (1973).

³R. R. Betts, H. T. Fortune, D. J. Pullen, and B. H. Wildenthal, in Argonne National Laboratory Physics Division Informal Report No. PHY-1972H, 1972 (unpublished), p. 342.

⁴L. Meyer-Schützmeister and D. S. Gemmell, Phys. Rev. Lett. **27**, 869 (1971).

⁵We are grateful to B. F. Bayman for having made this code available to us.

⁶J. R. Erskine and R. H. Vonderohe, Nucl. Instrum. Methods **81**, 221 (1970).

- ⁷L. Meyer-Schützmeister, J. W. Smith, G. Hardie, H. Siefkin, K. T. Knöpfle, M. Rogge, and C. Mayer-Böricke, Nucl. Phys. A199, 593 (1973).
- ⁸L. Meyer-Schützmeister, G. Hardie, and T. Sjoreen, Phys. Rev. C (to be published).
- ⁹Z. P. Sawa, J. Blomquist, and W. Gullholmer, Nucl. Phys. A205, 257 (1973).
- ¹⁰George H. Rawitscher and Shankar N. Mukherjee, Phys. Rev. 181, 1518 (1969).
- ¹¹R. Stock, R. Bock, P. David, H. H. Duhm, and T. Tamura, Nucl. Phys. A104, 136 (1967).
- ¹²J. J. Weaver, M. A. Grace, D. F. H. Start, R. W. Zurmühle, D. P. Balamuth, and J. W. Noé, Nucl. Phys. A196, 269 (1972).
- ¹³A. K. Dhar, D. R. Kulkarni, and K. H. Bhatt, Nucl. Phys. A238, 340 (1975).
- ¹⁴F. B. Malik and W. Scholz, Phys. Rev. 153, 1071 (1967).
- ¹⁵Gerald Hardie, David Gloeckner, L. Meyer-Schützmeister, and T. H. Braid, Phys. Rev. C 10, 1829 (1974).
- ¹⁶J. R. Comfort, H. T. Fortune, G. C. Morrison, and J. V. Maher, Phys. Rev. C 10, 2399 (1974).
- ¹⁷J. Kawa, J. Phys. Soc. of Jpn. 36, 929 (1974).
- ¹⁸F. G. Perey and G. R. Satchler, Nucl. Phys. A97, 515 (1967).
- ¹⁹L. McFadden and G. R. Satchler, Nucl. Phys. 84, 177 (1966).
- ²⁰M. S. Chowdhury and H. M. SenGupta, Nucl. Phys. A229, 484 (1974).
- ²¹T. T. S. Kuo and G. E. Brown, Nucl. Phys. A114, 241 (1968).
- ²²D. H. Gloeckner and R. D. Lawson, Phys. Lett. 53B, 313 (1974).